

# Unusual Behavior of the Ni<sup>1+</sup> moment and interstitial band in bi-infinite-layered La<sub>3</sub>Ni<sub>2</sub>O<sub>5</sub>F

Young-Joon Song<sup>1</sup>, Warren E. Pickett<sup>2</sup>, and Kwan-Woo Lee<sup>3,4</sup>

<sup>1</sup>*Institut für Theoretische Physik, Goethe-Universität Frankfurt,  
Max-von-Laue-Straße 1, 60438 Frankfurt am Main, Germany*

<sup>2</sup>*Department of Physics and Astronomy, University of California, Davis, California 95616, USA*

<sup>3</sup>*Division of Semiconductor Physics, Korea University, Sejong 30019, Korea*

<sup>4</sup>*Department of Applied Physics, Graduate School, Korea University, Sejong 30019, Korea*

(Dated: March 31, 2026)

## S1. NONMAGNETIC RESULTS

The nonmagnetic band structure within GGA is displayed in Fig. S1. For the  $pd\sigma$  bands in the 2D bi-layered square lattice, the Hamiltonian can be described by

$$\hat{H}(\mathbf{k}) = \begin{pmatrix} \epsilon(\mathbf{k}) & T_{\perp} \\ T_{\perp} & \epsilon(\mathbf{k}) \end{pmatrix}, \quad (1)$$

where the intralayer interaction is

$$\epsilon(\mathbf{k}) = \varepsilon_d + 2t_{100} [\cos(k_x a) + \cos(k_y a)] + 4t_{110} \cos(k_x a) \cos(k_y a) \quad (2)$$

with the on-site energy  $\varepsilon_d$ , and the interlayer interaction is

$$T_{\perp}(\mathbf{k}) = t_{001} + 4t_{111} \cos(k_x a) \cos(k_y a), \quad (3)$$

neglecting a tiny  $t_{101}$ . Applying this to the NM band structure yields  $\varepsilon_d = 87$  meV,  $t_{100} = -363$  meV,  $t_{110} = 94$  meV,  $t_{001} = 39$  meV, and  $t_{111} = -9$  meV. From the Hamiltonian, splittings between even-odd  $pd\sigma$  bands at each symmetry point are approximately  $2(t_{001} + 4t_{111})$  at the  $\Gamma$  ( $M$ ) and  $2(t_{001} - 4t_{111})$  at the  $X$ . So, the even-odd  $pd\sigma$  bands split most noticeably by  $\sim 150$  meV at the  $X$  point.

The fatband plots of the La1/La2  $5d$  and O  $p$  orbitals, enlarged in the range  $-1$  eV to  $1$  eV, are displayed in Fig. S2. Figure S3 provides the corresponding total and atom-projected densities of states. The features are described in the caption, note the gap between O/X  $2p$  states and the Ni  $3d$  bands around  $-2.3$  eV. The split van Hove singularities just below  $E_F$  are evident. For details, see the captions of these figures.

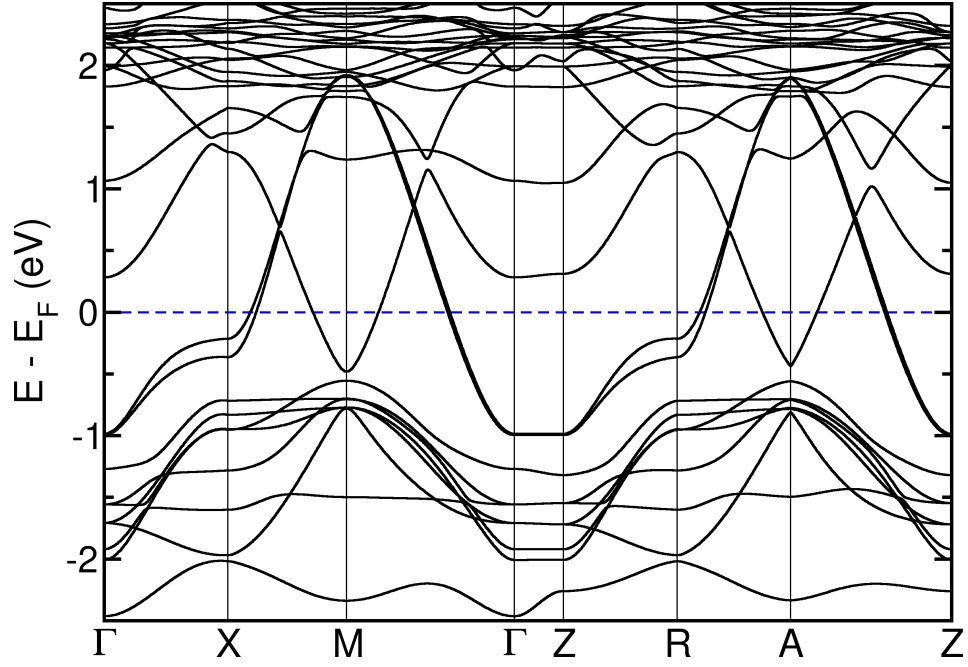


FIG. S1. Band structure for nonmagnetic  $\text{La}_3\text{Ni}_2\text{O}_5\text{F}$  with GGA, with a closer look at its interaction of the interstitial band with the Ni  $d$  bands. At the  $M$  point, a band from  $-0.8$  eV goes down, soon becoming linear along both symmetry directions for an eV or so. This band appears to be a continuation from the E-band (linear above, discussed in the text), which is just a little above, at  $M$  and at  $A$ . This identification is most pronounced at the  $A$  point, where the kink in the E-band is replicated by a kink in the band proceeding downward, which is a behavior unlike the smooth  $d$  bands. Possible connections are left for further study. The symmetry points follow those in the primitive tetragonal Brillouin zone (BZ), as given in the main text.

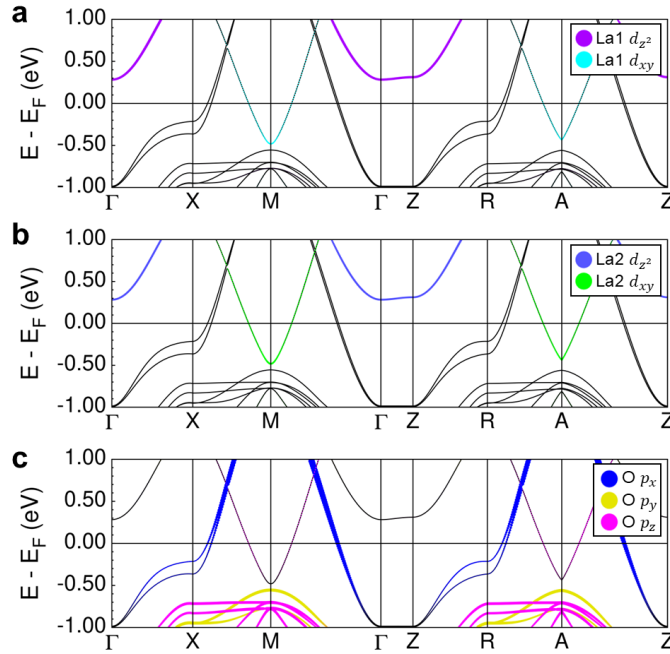


FIG. S2. Corresponding fatband plots of (a) La1  $5d$ , (b) La2  $5d$  (similar to La1), and (c) O  $2p$  for the O atom at  $(a/2, 0, 0)$  relative to Ni, in the range of  $-1$  to  $1$  eV. The  $k_z$  dispersion  $\Gamma - Z$  is negligible.

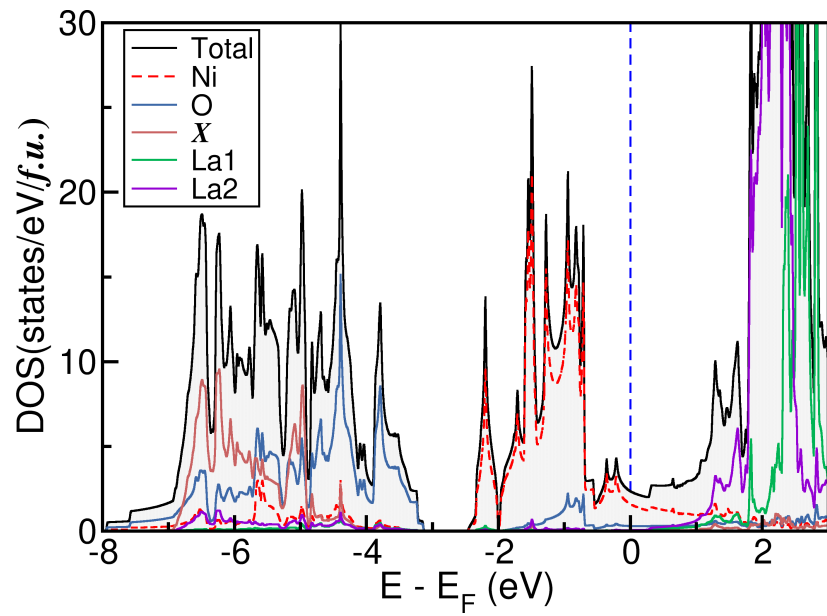


FIG. S3. Total and atom-projected densities of states (DOSs) for nonmagnetic  $\text{La}_3\text{Ni}_2\text{O}_5\text{F}$  with GGA, showing strong 2D features (jumps in the DOS). Estimating from the centers of each atom-projected DOS, the energy difference of Ni  $3d$  and O  $2p$  centers is about 4.5 eV, similar to that of  $\text{LaNiO}_2$ . At the Fermi energy  $E_F$  the DOS  $N(E_F)$  is 2.33 states/eV per f.u., consisting of about 65% Ni  $d$  states, 13% O  $2p$  states, 14% interstitial contributions, and a small remainder from other ions.

## S2. FERROMAGNETIC ALIGNMENT

The band structures of FM  $\text{La}_3\text{Ni}_2\text{O}_5\text{F}$  within GGA and GGA+U are given in Figs. S4 and S5, respectively. Figure S6 shows the corresponding DOSs.

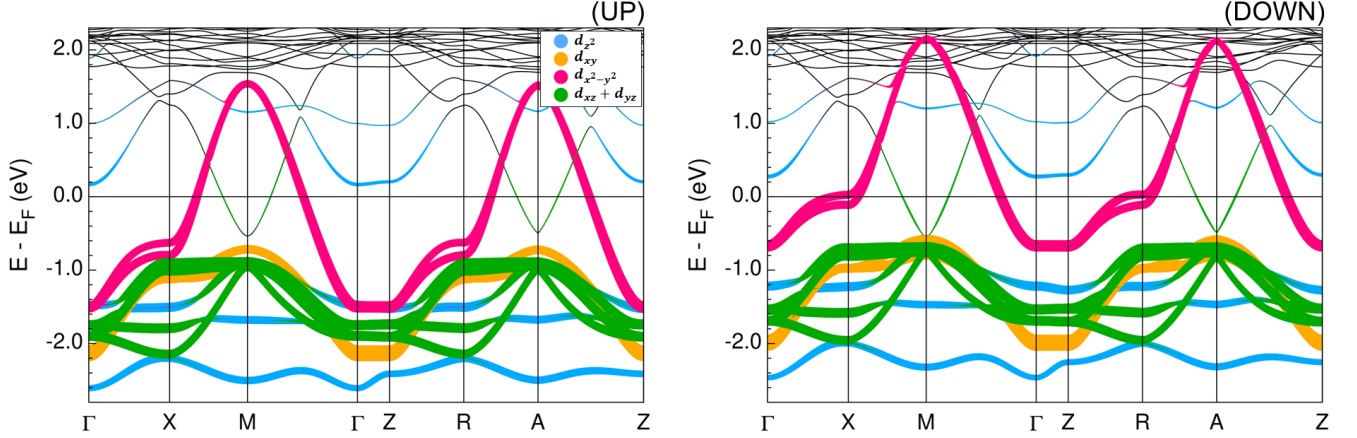


FIG. S4. GGA band structure of FM  $\text{La}_3\text{Ni}_2\text{O}_5\text{F}$ , in the range of  $-3$  to  $2$  eV, with the spin-up Ni  $3d$  fatbands plot on the left, the spin-down on the right. The exchange splitting is about  $0.7$  eV. Both the majority and minority  $3d_{x^2-y^2}$  orbitals of Ni are partially filled, leading to a small local moment of  $0.33 \mu_B/\text{Ni}$ .

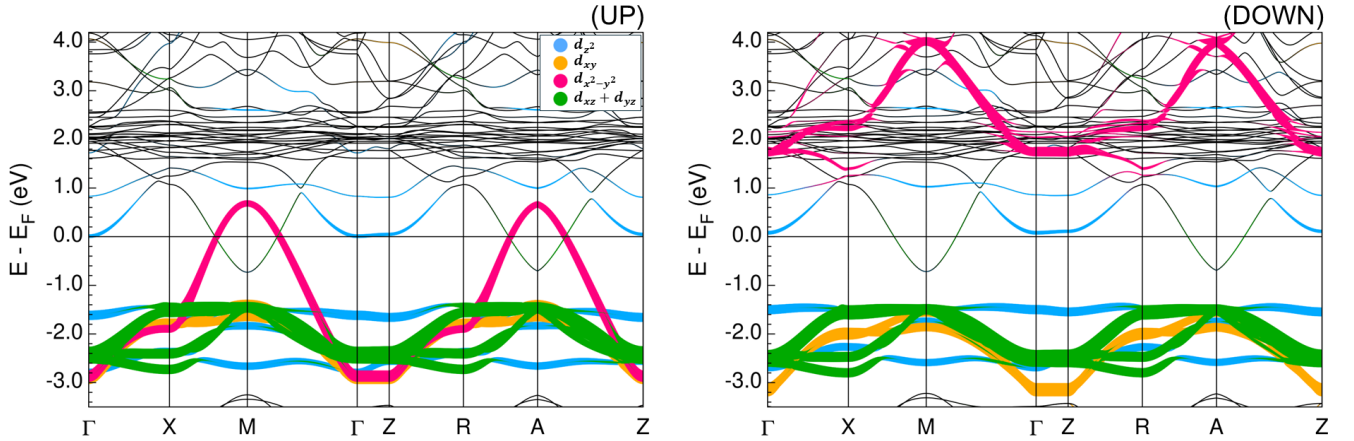


FIG. S5. Band structure (as in the previous figure) of FM  $\text{La}_3\text{Ni}_2\text{O}_5\text{F}$  within GGA+U ( $U_{eff} = 4$  eV) using the AMF double-counting scheme, with the overlaid Ni  $3d$  fatbands. The exchange splitting has been increased to  $\sim 4$  eV by this value of  $U_{eff}$ . Note: the  $M$ -centered electron and hole FSs remain unchanged even for  $U_{eff}$  up to  $5$  eV.

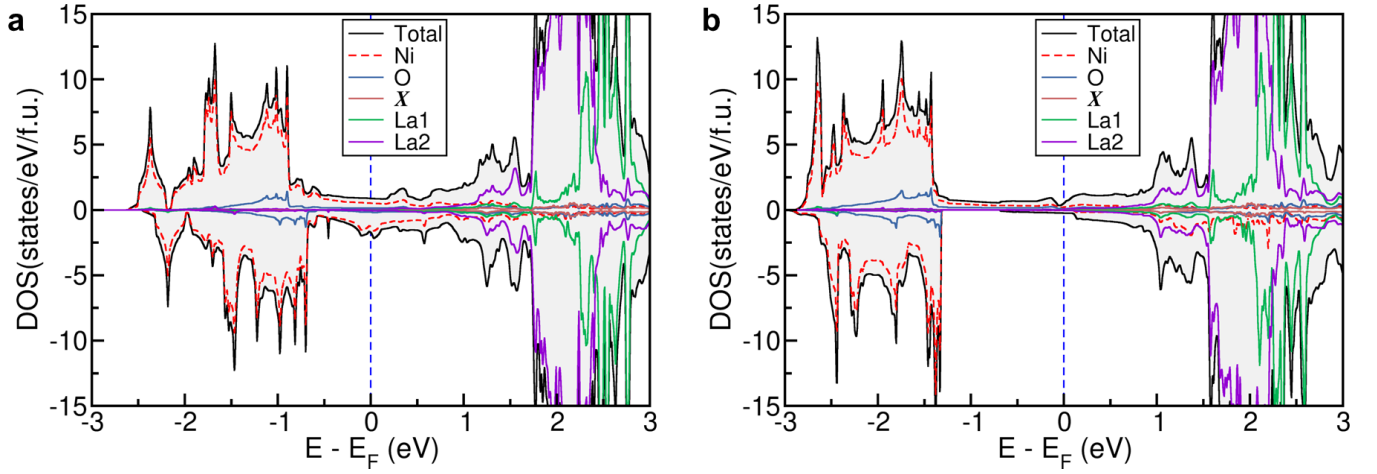


FIG. S6. Total and atom-projected densities of states (DOSs) of FM  $\text{La}_3\text{Ni}_2\text{O}_5\text{F}$  within (a) GGA and (b) GGA+U ( $U_{\text{eff}} = 3$  eV) using the AMF double-counting scheme. The difference is mainly the additional exchange (Mott) splitting given by  $U_{\text{eff}}$ .

### S3. ANTIFERROMAGNETIC ALIGNMENT

The GGA band structure of the G-AFM  $\text{La}_3\text{Ni}_2\text{O}_5\text{F}$  is shown in Fig. S7. Figure S8 shows the fatband plots of La ions and O ion. The 2D and 3D Fermi surfaces in GGA are described with orbital characters in Fig. S9. Additionally, the atom-projected DOSs within GGA+U at  $U_{\text{eff}} = 4$  eV appearing a small energy gap of 0.1 eV are provided in Fig. S10.

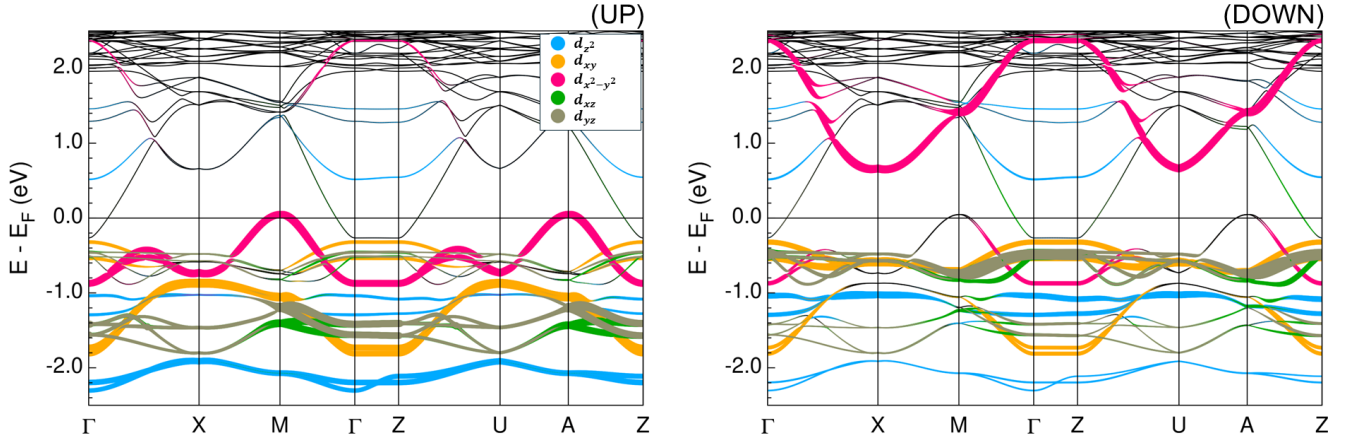


FIG. S7. Band structure of G-AFM  $\text{La}_3\text{Ni}_2\text{O}_5\text{F}$  within GGA, in the range of  $-2.5$  to  $2.5$  eV, emphasizing the Ni  $3d$  fatband plots for (left) majority and (right) minority characters. The filled majority Ni  $d_{x^2-y^2}$  band lies below  $E_F$ , while the unfilled minority counterpart is broadened into  $0.5$  to  $2.5$  eV range, mixing with upper conduction bands. The exchange splitting of the Ni  $3d_{x^2-y^2}$  band centers is  $\sim 2$  eV.

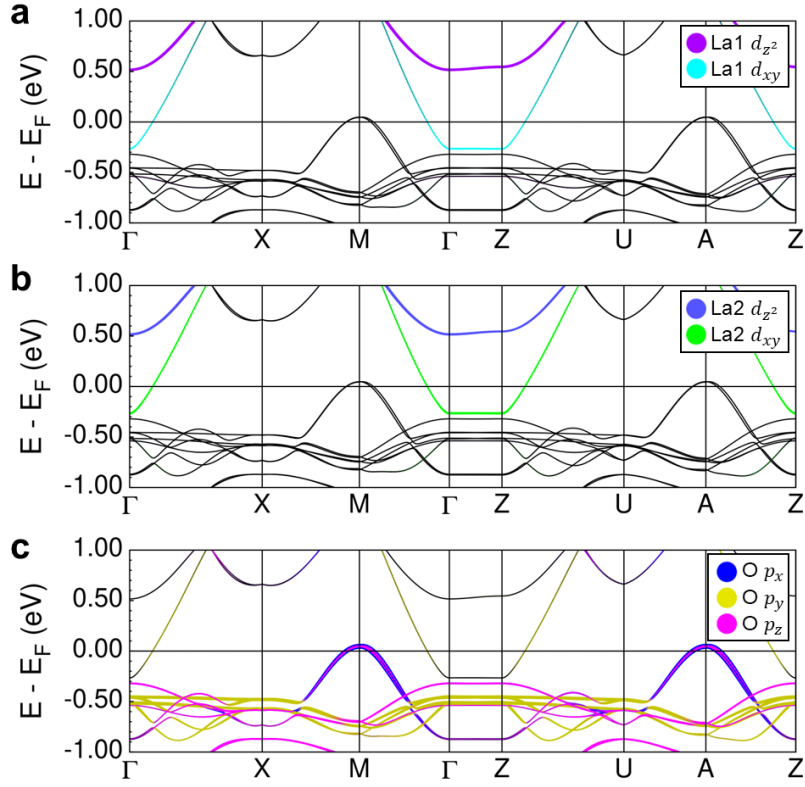


FIG. S8. Fatband plots of (a) La1  $5d$ , (b) La2  $5d$ , and (c) O  $2p$  for the G-AFM  $\text{La}_3\text{Ni}_2\text{O}_5\text{F}$  within GGA, enlarged in the range of  $-1$  eV to  $1$  eV. The “upper Hubbard band” with O  $p_\sigma$  character, lies above the range of this plot.

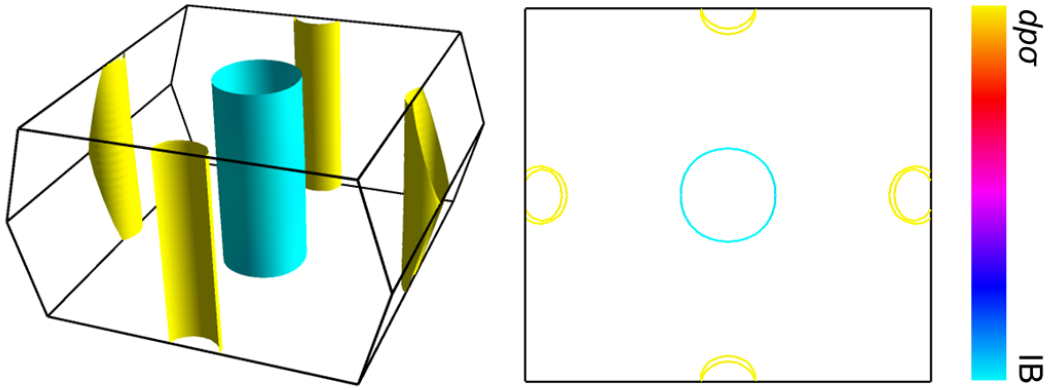


FIG. S9. Fermi surfaces of the G-AFM  $\text{La}_3\text{Ni}_2\text{O}_5\text{F}$  in GGA, showing extreme 2D character. The  $\Gamma$ -centered tube contains interstitial electrons (folded back from the NM  $M$  point), while the two  $M$ -centered tubes contain holes, reflecting near compensation.

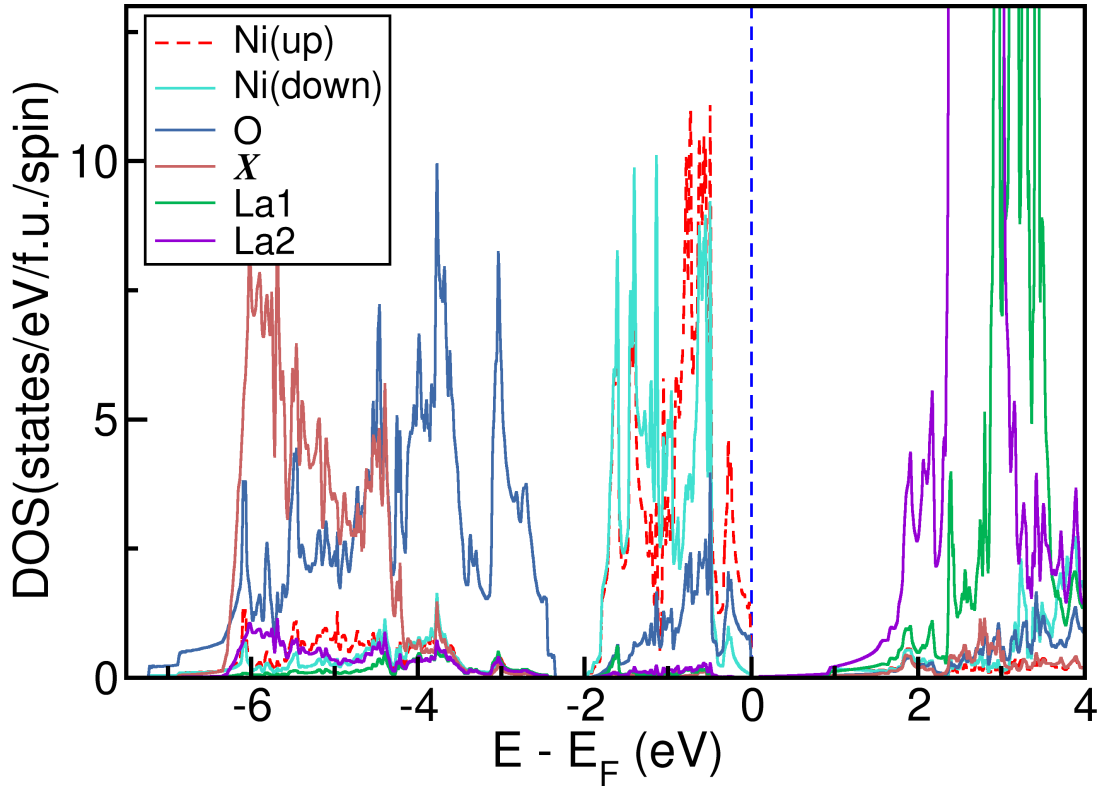


FIG. S10. Atom-projected DOSs of the G-AFM  $\text{La}_3\text{Ni}_2\text{O}_5\text{F}$  within GGA+U ( $U_{eff} = 4$  eV), in the full energy range, showing a small energy gap of  $\sim 0.1$  eV, not visible on this scale. Most  $Xp$  orbitals are located in the energy range from  $-6.2$  to  $-4.2$  eV, while the  $O p$  orbitals span from  $-7.2$  to  $-2.3$  eV. These  $O p$  orbitals are separated from the Ni  $d$  orbitals due to crystal field splitting and to the  $pd\sigma$  hybridization.